

# Emissions of 1,3-Dichloropropene and Chloropicrin after Soil Fumigation under Field Conditions

Scott R. Yates,<sup>\*,†</sup> Daniel J. Ashworth,<sup>†,‡</sup> Wei Zheng,<sup>‡,Δ</sup> Qiaoping Zhang,<sup>†</sup> James Knuteson,<sup>§,Π</sup> and Ian J. van Wessenbeeck<sup>§</sup>

<sup>†</sup>U.S. Salinity Laboratory, USDA-ARS, 450 West Big Springs Road, Riverside, California 92507, United States

<sup>‡</sup>Department of Environmental Sciences, University of California, Riverside, California 92521, United States

<sup>§</sup>Dow Agrosciences, Indianapolis, Indiana 46268, United States

## S Supporting Information

**ABSTRACT:** Soil fumigation is an important agronomic practice in the production of many high-value vegetable and fruit crops, but the use of chemical fumigants can lead to excessive atmospheric emissions. A large-scale (2.9 ha) field experiment was conducted to obtain volatilization and cumulative emission rates for two commonly used soil fumigants under typical agronomic practices: 1,3-dichloropropene (1,3-D) and chloropicrin. The aerodynamic method and the indirect back-calculation method using ISCST3 and CALPUFF dispersion models were used to estimate flux loss from the treated field. Over the course of the experiment, the daily peak volatilization rates ranged from 12 to 30  $\mu\text{g m}^{-2} \text{s}^{-1}$  for 1,3-D and from 0.7 to 2.6  $\mu\text{g m}^{-2} \text{s}^{-1}$  for chloropicrin. Depending on the method used for quantification, total emissions of 1,3-D and chloropicrin, respectively, ranged from 16 to 35% and from 0.3 to 1.3% of the applied fumigant. A soil incubation study showed that the low volatilization rates measured for chloropicrin were due to particularly high soil degradation rates observed at this field site. Understanding and quantifying fumigant emissions from agricultural soil will help in developing best management practices to reduce emission losses, reducing adverse impacts to human and ecosystem health, and providing inputs for conducting risk assessments.

**KEYWORDS:** soil fumigation, volatilization, emissions, Telone C-35, 1,3-dichloropropene, chloropicrin, bare soil, field experiment, shank injection, Industrial Source Complex Short-Term model (ISCST3), CALPUFF dispersion model, aerodynamic gradient method

## INTRODUCTION

Soil fumigation can significantly affect regional air quality.<sup>1</sup> Soil fumigation can lead to toxic substances entering the regional air stream as well as increasing the concentration of potential precursors for photochemical smog, which is formed by the reaction of volatile organic chemicals with nitrogen oxides in the atmosphere. Photochemical smog has become a problem in California during the summer months, and fumigants have been identified as potential precursors. Monitoring indicates that additional efforts are needed to ensure that U.S. EPA's 8-h ozone standard<sup>2</sup> is attained throughout the state.

The fumigant 1,3-dichloropropene (1,3-D) is an effective nematicide used for preplant soil fumigation; however, it is considered a possible carcinogen and is a Clean Air Act substance.<sup>3</sup> The high volatility (vapor pressure = 4.3 kPa<sup>4</sup>) of 1,3-D facilitates its movement, which increases effectiveness, but may also lead to high atmospheric emissions<sup>3,5</sup> and the potential for worker exposure.<sup>6</sup> In 1990, the detection of high 1,3-D concentrations in ambient air samples at multiple sites in California led to a suspension of 1,3-D as a soil fumigant.<sup>7</sup> The suspension remained in effect until 1995, when approaches to mitigate emissions were developed and tested.

Chloropicrin (trichloronitromethane) is effective for controlling soilborne fungi, diseases, and nematodes and was first registered in the United States in 1975.<sup>8</sup> Significant emissions for chloropicrin are possible after soil fumigation due to its high vapor pressure (2.4 kPa<sup>4</sup>). Chloropicrin has been found to be a reactive compound that promotes tropospheric ozone for-

mation if present with other reactive organic compounds in the atmosphere.<sup>9</sup> Even though chloropicrin has been used in soil fumigation for decades, there is much to learn about its fate and persistence in soil and its volatilization from soil into the atmosphere.<sup>10</sup> More importantly, there is a great need to develop methods to control emissions for all soil fumigants.

There is very little published information on field-scale emissions of 1,3-D or chloropicrin. There have been several reported soil column experiments<sup>11–18</sup> that placed 1,3-D emission losses from bare soil in the range of 20–77% of the applied dosage. These studies also revealed that emission rates obtained using laboratory soil columns can have high variability (i.e.,  $\mu = 41\%$ ,  $\sigma = 16\%$ ). Total emission rates have been obtained under field conditions using micrometeorological and flux chamber methods. These studies have shown a similar range in total emissions of 12–80%,<sup>19–25</sup> with the highest estimates obtained using flux chambers ( $\mu = 56\%$ ,  $\sigma = 22\%$ ). Flux chambers offer a relatively simple and cost-effective method for determining emission rates. They are also known to suffer from several practical problems, such as sampling a small surface area and the presence of the chamber affecting the tested surface,<sup>26</sup> which can affect the results. Total emission estimates of chloropicrin based on laboratory soil column

Received: March 19, 2015

Revised: May 13, 2015

Accepted: May 22, 2015

Published: May 22, 2015

experiments place losses in the range of 7–16% of applied fumigant.<sup>16,18</sup> For measurements utilizing flux chambers,<sup>24</sup> the total losses were reported to be 30%.

It is imperative to better understand emissions from fumigated soil at typical agronomic scales to reduce the adverse impacts from soil fumigation. Large-scale field measurement of fumigant emissions provides information regulators require at the appropriate scale while serving as a reference baseline for the development and testing of new methods to reduce emissions.

Continued use of 1,3-D and chloropicrin will likely require extensive information on their environmental fate and transport collected at agronomic scales. The objective of this study was to conduct a field experiment to obtain needed information on the period-averaged and total emissions of 1,3-D and chloropicrin after shank fumigation in a large-scale agricultural field. Emission information is required by state and federal regulators as inputs into risk assessment models for the development of buffer zones to ensure public safety and also benefits the agricultural community by providing science-based information concerning rates of emission.

## ■ EXPERIMENTAL METHODS

The 2007 field experiment was conducted in an agricultural field near Buttonwillow, CA, USA, from September 5 to 21. The field soil was classified as Milham sandy loam (fine-loamy, mixed, thermic Typic Haplargids) and had approximately 1% organic matter content in the upper 10 cm, which decreased with depth. Approximately 2 weeks before the start of the experiment, the field was plowed and disked to break up any large soil aggregates and irrigated so that the soil condition was suitable for fumigation, with a water content of approximately 0.2 (cm<sup>3</sup> cm<sup>-3</sup>). Telone C-35, a mixture of 1,3-D (68.1%) (CAS Registry No. 542-75-6) and chloropicrin (31.9%) (CAS Registry No. 76-06-2) was provided by Dow Agrosciences (Indianapolis, IN, USA) and applied by a commercial applicator using standard fumigation practices. 1,3-D contains two isomers, *cis*-1,3-D and *trans*-1,3-D, in a 50:50 ratio. The fumigation began at 9:35 a.m. (*t* = 0.40 day) and was completed within 3 h. The injection rig carried a 450 cm tool bar with nine shanks spaced in 50 cm increments laterally across the tool bar. The target depth of application was 46 cm (18 in.), and the fumigant material was applied to a nearly square 2.9 ha area (162 × 178 m). The target application rate was 240 kg/ha (20 gal/acre), and the actual weight of Telone C-35 applied was determined after fumigation (474.5 kg of 1,3-D and 222.3 kg of chloropicrin).

### Measurement of 1,3-D and Chloropicrin Concentration.

Atmospheric samples of 1,3-D and chloropicrin were obtained using XAD-4 tubes (SKC 226-175, SKC, Inc., Fullerton, CA, USA) followed by a charcoal backup tube (SKC 226-09, SKC, Inc.) to check for 1,3-D breakthrough both in laboratory and field samples. Ambient air was pulled through the sampling tube at a nominal rate of 150 cm<sup>3</sup>/min using a vacuum system.

The 1,3-D and chloropicrin concentrations in the atmosphere were collected at 1.5 m above the soil surface at 12 locations surrounding the field site (see Supporting Information, Figure S1). Sample collection began at 8:00 a.m. (i.e., *t* = 0.33 day) and consisted of 3-h samples during the daytime and a 12-h sample at night. The daytime sampling intervals were increased to 6 and 12 h beginning on days 4 and 10, respectively. Sampling periods were lengthened to ensure that sufficient mass was collected in the sampling tubes for residue analysis as the experiment progressed.

Additional samples of the 1,3-D and chloropicrin concentrations in the atmosphere were collected at 10, 40, and 80 cm above the ground surface at the center of the treated field for use in a direct method of estimating mass flux because a concentration gradient is required. During days 0–5, the measurement periods were 2 h long during daytime and a single nighttime sample was collected. The daytime

sampling intervals were increased to 3, 4, and 6 h beginning on days 5, 9, and 12, respectively.

**Meteorological Measurements.** Wind speed measurements were obtained at 20, 40, 80, and 160 cm above the ground surface using Windsonic 2-D sonic anemometers (Gill Instruments, Ltd.). Fine-wire thermocouples (FW3, Campbell Scientific, Inc.) were placed at 10, 40, and 80 cm above the ground surface to measure the air temperatures and temperature gradient. Relative humidity and temperature (1.5-m height, CS-215, Campbell Scientific, Inc.), net radiation (1-m height, Q-6, Radiation and Energy Balance Systems, Inc.), and barometric pressure (Vaisala PTA-427, Campbell Scientific, Inc.) measurements were also obtained during the experiment. These sensors were located at field center (see the Supporting Information).

Wind speed, wind direction (Wind Monitor, 5305, R. M. Young, Traverse City, MI, USA), and solar radiation (LI-200S, LI-COR, Inc.) were measured at 10-m height, which was positioned in a nearby field. Hourly averaged solar and net radiation measurements were collected yielding a nominal time series of 384 values (i.e., 24 h × 16 daily values). The average and standard deviation were calculated for each hour of the day to represent a typical daily cycle. This resulted in 24 average solar and net radiations and their standard deviations.

**Methods for Measuring the Volatilization Rate.** Two regulatory approaches were used to obtain the volatilization rate. A back-calculation method using the Industrial Source Complex Short-Term model (ISCST3),<sup>27,28</sup> has been extensively used for regulatory decisions by the California Department of Pesticide Regulations (CDPR) since the 1990s.<sup>29</sup> A different air dispersion model, CALPUFF,<sup>30</sup> was also used. EPA has recently adopted AERMOD<sup>31</sup> as a replacement for ISCST3. In California, due to the extensive historical use and past decisions based on ISCST3, CDPR has not required or recommended use of AERMOD for determining emission estimates from field application. CDPR evaluated AERMOD and found that the new functionality in AERMOD was not related to the area-source components of the model, and therefore replacement of ISCST3 was not warranted.<sup>29</sup>

The emission rates obtained using the back-calculation method involve comparing observed ambient concentrations in the atmosphere surrounding the field to concentrations calculated using an atmospheric dispersion model (e.g., ISCST3 or CALPUFF). The estimated emission rate is obtained by adjusting the ISCST3 model emission rate to produce the best fit to the measured concentration values (i.e., back-calculating the field emission rate).

The estimated emission rate is based on a linear relationship

$$C_{\text{meas}} = b + EC_{\text{ISC}} \quad (1)$$

where  $C_{\text{meas}}$  is the measured ambient concentration,  $E$  is the unknown actual emission rate,  $b$  is a background concentration that occurs when  $E = 0$ , and  $C_{\text{ISC}}$  is a predicted concentration at the receptor. The model parameters are estimated by linear regression using observed ambient concentrations ( $C_{\text{meas}}$ ) at locations surrounding the treated field and the predicted concentrations ( $C_{\text{ISC}}$ ) at each sampling location obtained using an atmospheric dispersion model with a nominal emission rate ( $E_{\text{nom}}$ ). Because the ISCST3 or CALPUFF concentrations are proportional to the unknown emission rate,  $E$  can be estimated from

$$\text{flux} = E = mE_{\text{nom}} \quad (2)$$

where the intercept,  $b$ , and the slope,  $m$ , are obtained from linear regression.

All dispersion model simulations used in back-calculation methods used the regulatory default options, rural dispersion, flat terrain, receptor height of 1.5 m, and meteorological inputs using standard methodology.<sup>30</sup> For CALPUFF simulations, the field was split into four quadrants, and fumigant movement and dispersion were followed from each quadrant to the receptors.

For comparison purposes, the aerodynamic method (ADM)<sup>32</sup> was also used to estimate the volatilization rate based on gradients of wind speed, temperature, and fumigant concentration<sup>32</sup> collected over a relatively large and spatially uniform source area. It is customary to place the instruments at heights that are approximately 1–2% of the upwind fetch distance, which for this experiment would be heights up

to 80 cm. The air concentrations at the 80-cm height were found to be unreliable due to an equipment malfunction; therefore, volatilization rates were calculated using the 10 and 40 cm data. More information is provided in the Supporting Information.

The total fumigant mass lost after application, mass, was calculated using

$$\text{mass} = \text{area} \sum_n f_z(t_i) \Delta t_i \quad (3)$$

where  $f_z(t_i)$  is the  $i$ th period volatilization rate ( $\mu\text{g m}^{-2} \text{s}^{-1}$ ),  $\Delta t_i$  is the time interval for period  $i$ ,  $n$  is the total number of periods, and area is the area ( $\text{m}^2$ ) of the treated region of the field.

**Chemical Analysis.** Chemical analyses followed the same procedures described in Yates et al.<sup>33</sup> In brief, the concentrations of 1,3-D and chloropicrin in solvent extracts were determined by gas chromatography (GC) using an HP 6890 GC (Agilent Technologies, Palo Alto, CA, USA) equipped with an electron capture detector (ECD). The GC conditions were as follows: use of a 30 m  $\times$  0.25 mm  $\times$  1.4  $\mu\text{m}$  DB-VRX capillary column (J&W Scientific, Folsom, CA, USA) with 240  $^{\circ}\text{C}$  inlet temperature, 290  $^{\circ}\text{C}$  detector temperature, and 1.6  $\text{cm}^3 \text{min}^{-1}$  column flow rate (He).

## RESULTS

**Environmental Conditions.** Shown in Figure 1 are hourly means and standard deviations of the solar irradiance ( $Q_{\text{in}}$ ) and

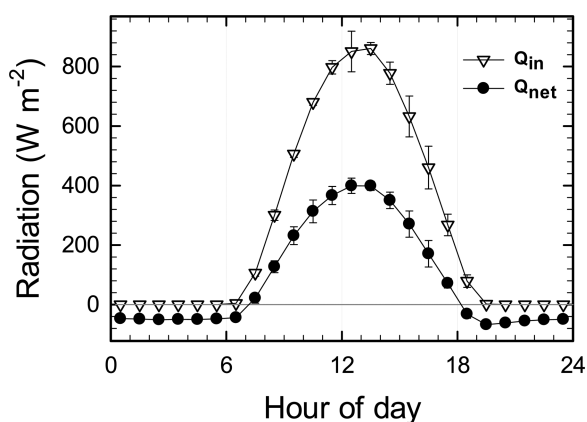


**Figure 1.** Global solar irradiance ( $\text{W m}^{-2}$ ) and net radiation ( $\text{W m}^{-2}$ ) as a function of time of day. The point values are averages of the hourly radiation over the entire experiment, and the error bars are the standard deviations. Small standard deviations are indicative of relatively uniform clear sky conditions throughout the experiment.

net solar radiation ( $Q_{\text{net}}$ ). The maximum and average solar flux densities were 861 and 264  $\text{W m}^{-2}$ , respectively. The maximum standard deviation was 72  $\text{W m}^{-2}$  and occurred at 5:00 p.m.

The net radiation was also found to be piecewise smooth during the daytime and was highly uniform at a given time of day during this experiment. The maximum, minimum, and average values were 399,  $-67$ , and 86  $\text{W m}^{-2}$ , respectively. The maximum standard deviation for the 24 periods was 44  $\text{W m}^{-2}$ .

During the first 8 days of the experiment, the daily maximum temperatures at 1.5 m were similar and ranged from approximately 32 to 35  $^{\circ}\text{C}$  and averaged 33.2  $^{\circ}\text{C}$  (Figure 2A). The daily minimum temperature varied from 15 to 20  $^{\circ}\text{C}$  and averaged 17.3  $^{\circ}\text{C}$ . Starting at day 8, daily maximum temperatures were more variable, ranging from 22 to 31  $^{\circ}\text{C}$ , and averaged 27.3  $^{\circ}\text{C}$ , and the daily minima varied from 12 to 15  $^{\circ}\text{C}$  and averaged 13.1  $^{\circ}\text{C}$ .

The hourly averaged wind speed at 10 m height had a maximum of 5.2  $\text{m s}^{-1}$ , and the daily peak 1-h wind speeds had

an average and standard deviation of  $3.2 \pm 0.8 \text{ m s}^{-1}$  (Figure 2B). During the nighttime, the daily minimum wind speeds averaged 0.64  $\text{m s}^{-1}$  ( $\pm 0.32$ ), and five values (1.5%) were below 0.5  $\text{m s}^{-1}$ , below the starting threshold for the 10-m wind direction sensor.

The wind-rose diagram that summarizes the frequency distribution of the wind speed and direction during the experiment suggests the winds were predominately from the northwest and that there was more variation in wind direction at 10 m compared to measurements taken at the center of the field (1.6 m) (Figure 3). This diagram uses 1- or 2-min averaged wind speed and wind direction data and shows that occasionally winds in excess of 5  $\text{m s}^{-1}$  were observed. The length of each wedge provides the frequency that the winds came from that particular direction interval, per unit time. The color sections on each wedge provide frequency information about the wind speed ranges. For example, at 10 m, for approximately 14% of the time during the experiment, the winds were blowing from the north (i.e.,  $360^{\circ} \pm 11.25^{\circ}$ ) and about 3.2% of the time the wind speed was within the range of 2.0–2.5  $\text{m s}^{-1}$  (i.e., 6.7% – 3.5%). For these short time interval measurements, (i.e., 1–2 min averaging), the maximum observed wind speed was 8.3  $\text{m s}^{-1}$ , 1.6% of the measurements exceeded 5  $\text{m s}^{-1}$ , and 4.5% were  $<0.5 \text{ m s}^{-1}$ .

**Air Concentrations.** One air monitoring station was placed 50 m northeast of the field due to a fenced property boundary, and the remaining 11 stations were positioned 30, 90, or 120 m from the field edge. Figure 4 shows the maximum concentrations of *cis*-1,3-D, *trans*-1,3-D, and chloropicrin from the 11 monitoring stations surrounding the field. During periods with steady wind direction, the up-wind air samplers recorded concentrations that were below detectable levels. In general, the highest concentrations occurred during nighttime or early morning hours.

For *cis*-1,3-D, the maximum daily concentrations at the center of the field at height 0.4 m exceeded 1000  $\mu\text{g m}^{-3}$  14 h after the fumigation was completed. Fumigant labels typically specify a field re-entry period and a buffer setback from the field edge to minimize the potential for bystander exposure. High concentration levels were also observed before sunrise on days 3 (657  $\mu\text{g m}^{-3}$ ) and 4 (840  $\mu\text{g m}^{-3}$ ). At a distance of 30 m from the field boundary, the daily peak *cis*-1,3-D concentration exceeded 60  $\mu\text{g m}^{-3}$  during the first 2 days after application and the maximum concentrations occurred on days 3–4 (109–112  $\mu\text{g m}^{-3}$ ). At greater distances, daily maximum *cis*-1,3-D concentrations were approximately 30 and 35% lower than at 30 m. During the first 24 h after fumigation, the concentrations of *trans*-1,3-D were about 65% less than the *cis*-1,3-D isomer, approximately 20% less than *cis*-1,3-D values for days 3 and 4. After 4 days, *cis*- and *trans*-1,3-D concentrations were similar in magnitude ( $<10\%$  difference).

Chloropicrin concentrations were generally very low, especially after the first 24 h. The maximum on-field concentration was 60  $\mu\text{g m}^{-3}$  and 15, 13, and 7  $\mu\text{g m}^{-3}$ , respectively, at distances of 30, 90, and 120 m from the field boundary. After approximately 4 days, the maximum chloropicrin concentration levels surrounding the field were low ( $<1 \mu\text{g m}^{-3}$ ), and after 9.54 days, sampling for chloropicrin ended.

**Fumigant Emissions.** Transient 1,3-D and chloropicrin volatilization rates using the ISCST3 and CALPUFF methods are shown in Figure 5; the maximum flux rates, the maximum 24-h average flux rates, and the percent total emissions for the



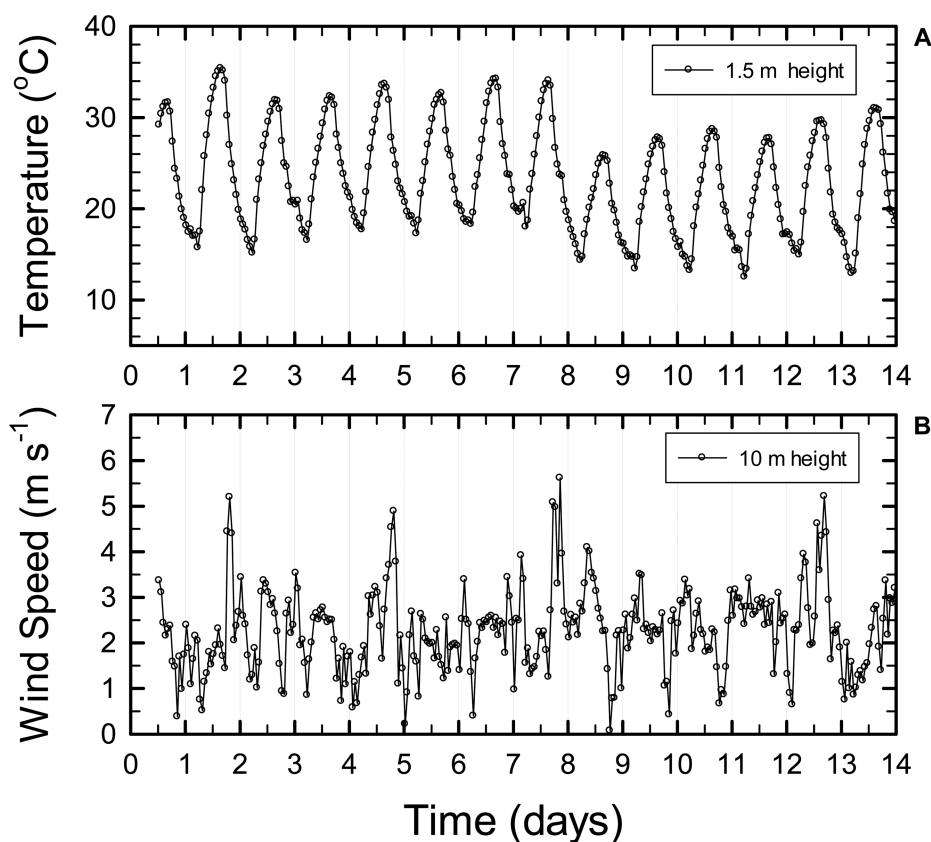


**Figure 2.** (A) Air temperature ( $^{\circ}\text{C}$ ) at 1.5 m and (B) wind speed ( $\text{m s}^{-1}$ ) at 10 m above the soil surface during the experiment. Integer values occurred at midnight, and each point is a 1-h sample average.

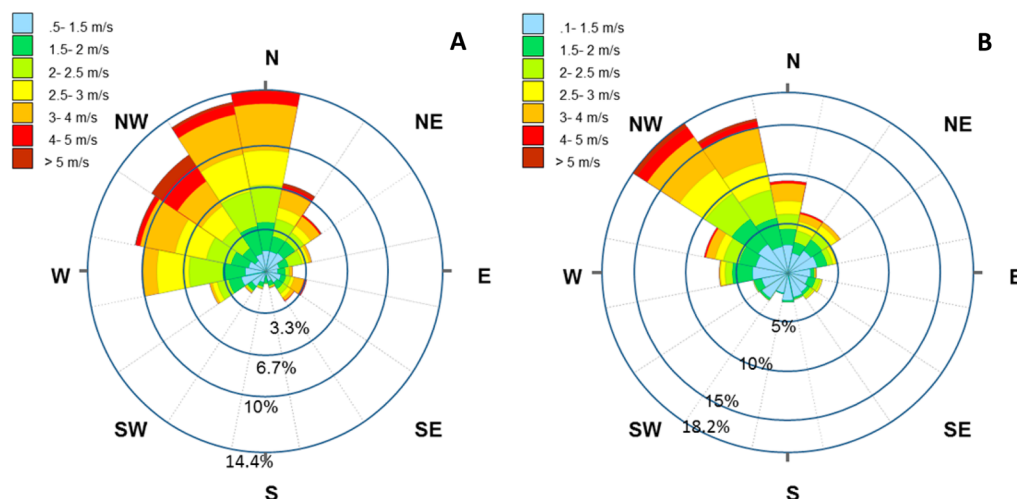


**Figure 3.** Wind rose diagrams showing the wind direction, wind speed, and frequency that the wind occurred in a specific direction. Two-minute averaged wind speed and direction were used in (A) and 1-min averaged wind speed and direction in (B). In (A), wind measurements at 10 m are shown. In (B), wind measurement at 1.6 m and at field center are shown.

three measurement methods are summarized in Table 1. For CALPUFF and ISCST3, the maximum flux rate for 1,3-D occurred at day 2, and for chloropicrin it occurred during fumigant application. The shaded areas in Figure 5 are the 24-h average flux rates calculated by converting the total mass lost for each day, using CALPUFF, into a flux density. Averaging smooths the short-term fluctuations and more clearly reveals the underlying behavior. The volatilization rates using the ISCST3 model were consistently less than those found using the CALPUFF model. For *cis*-1,3-D and *trans*-1,3-D, the

maximum and average ISCST3 flux rates were 59–63% less than CALPUFF rates and for chloropicrin, 74–85% less. For the CALPUFF method, the estimated total volatilization of *cis*-1,3-D, *trans*-1,3-D, and chloropicrin, respectively, was 32, 23, and 0.9% (Table 1). For the ISCST3 model, the estimated total volatilization, respectively, was 19, 13, and 0.3%.

Figure 6 shows time series for 1,3-D and chloropicrin volatilization rates obtained with the aerodynamic method. The maximum emission rates for *cis*-1,3-D, *trans*-1,3-D, and chloropicrin, respectively, were 18, 9.2, and  $0.68 \mu\text{g m}^{-2} \text{s}^{-1}$

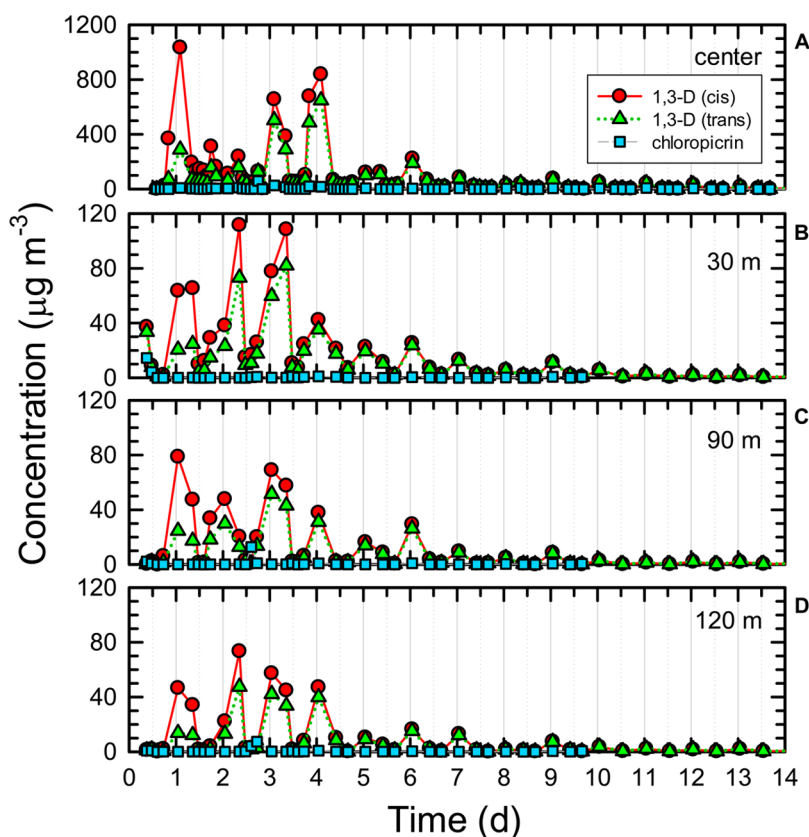


**Figure 4.** Maximum 1,3-D isomer and chloropicrin concentrations in air at samplers located 30, 90, and 120 m from the edge of field plots (see Supporting Information, Figure S1). Measurements were taken 1.5 m above the soil surface. Time scale begins at midnight September 5, 2007.

(Table 1). For *cis*-1,3-D, the maximum emission rate was within 2% of the back-calculated value using CALPUFF and for *trans*-1,3-D, within 22%. The aerodynamic method yielded total emission estimates of 42, 28, and 1.3% for *cis*-1,3-D, *trans*-1,3-D, and chloropicrin, respectively (Table 1). The aerodynamic method estimates of total emission for *cis*-1,3-D, *trans*-1,3-D, and chloropicrin, respectively, were 33, 25, and 49% higher compared to the back-calculation method using the CALPUFF air dispersion model.

## DISCUSSION

**Wind Speed, Temperature, and Radiation.** Warm temperatures, cloudless conditions, and persistent wind directions are typical weather patterns in the southern San Joaquin Valley in August and September,<sup>33</sup> but wind speeds that produce windblown dust were not observed during the field study. During high wind speeds, windblown dust can reduce visibility and energy inputs, which could affect fumigant emissions. Measurements of solar radiation obtained during a previous experiment that was conducted in late August and early September 2005<sup>33</sup> produced a similar curve as Figure 1, but with slightly lower standard deviations for  $Q_{in}$  at 11:00 a.m. and in the early afternoon. The overall low standard deviations shown in Figure 1 indicate that consistent energy inputs were observed during this field experiment and, for comparative purposes, that environmental conditions were similar to a previous experiment conducted in 2005.<sup>33</sup>

Wind speed measurements collected in 2005 in the vicinity of the field experiment using research grade cup anemometers (CWT-1806, C. W. Thornthwaite Associates)<sup>33</sup> indicated that northerly and westerly wind directions are common to this

region of California and align with the general orientation of the San Joaquin Valley and surrounding mountains.<sup>33</sup> In 2005, 93% of hourly wind speed measurements during August and September were below  $3 \text{ m s}^{-1}$  with a maximum of  $5.6 \text{ m s}^{-1}$  and were predominately from the north-northwest. During this experiment, 78% of the hourly wind speeds were below  $3 \text{ m s}^{-1}$  and the maximum was  $5.6 \text{ m s}^{-1}$  (day 8). The average was  $2.3 \text{ m s}^{-1}$ , the minimum was  $0.07 \text{ m s}^{-1}$  (day 9), and only six periods were below  $0.5 \text{ m s}^{-1}$  and only two periods below  $0.25 \text{ m s}^{-1}$ . Wind direction measured at 1.6 m near the center of the field show similar, but much more consistent, wind direction. This could be partly due to the on-field sensor type, which was a 2-D sonic anemometer consisting of no moving parts and with a threshold measurement of  $<0.01 \text{ m s}^{-1}$ . The mechanical wind direction sensor (10 m) may have been affected by wind buffeting, stalling, and overshoot compared to a high-frequency, nonmechanical device (1.6 m). Even though the field site was flat and had a large uniform surface surrounding the site, near-surface wind directions might also be affected by local topographic effect compared to higher elevation measurements.

**Air Concentrations.** In general, the highest concentrations occurred during nighttime and early morning hours; this is generally interpreted as a consequence of a stable atmosphere and lower turbulence.<sup>34</sup> The stability of the atmosphere can be estimated from the temperature and wind speed at two heights by calculating the gradient Richardson's number,  $R_i$ , and using  $R_i$  in an empirical relationship for atmospheric stability,  $\Phi_m$  (see the Supporting Information). These relationships are described and shown in Figure S2 for a height of 0.6 m. For neutral stability  $\Phi_m \approx 1$ . Values of  $\Phi_m > 1$  indicate a stable atmosphere, which occurred during nighttime and early morning hours of

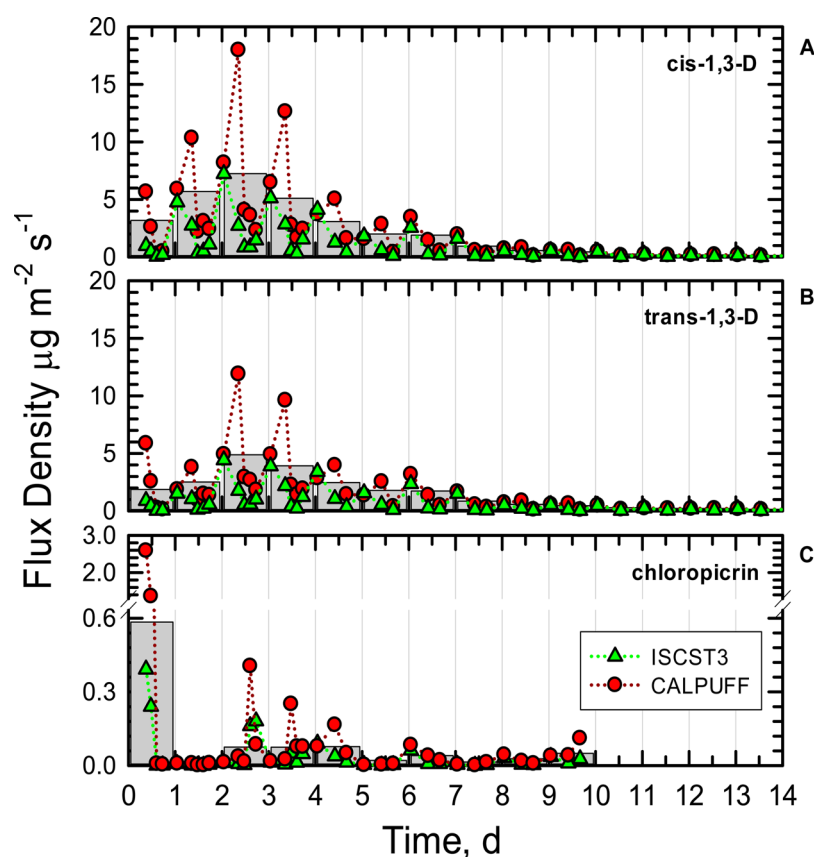


**Figure 5.** Volatilization rate (i.e., flux density,  $\mu\text{g m}^{-2} \text{s}^{-1}$ ) as a function of time (day) after application for the CALPUFF v6 (circles) and ISCST3 (triangles) methods. Shaded areas are mass losses for each day (CALPUFF) converted into daily averaged volatilization rates. For day 0, the shaded area is based on 16 h of available data.

**Table 1.** Fumigant Mass Applied, Maximum Flux Rate during Experiment, Maximum 24-h Average Flux Rate, and Total Emissions for Several Fumigants and Flux Measurement Methods

fumigant or formulation	appld mass (kg)	CALPUFF			ISCST3			ADM		
		max flux ( $\mu\text{g m}^{-2} \text{s}^{-1}$ )	max 24-h av ( $\mu\text{g m}^{-2} \text{s}^{-1}$ )	total emissions (%) <sup>a</sup>	max flux ( $\mu\text{g m}^{-2} \text{s}^{-1}$ )	max 24-h av ( $\mu\text{g m}^{-2} \text{s}^{-1}$ )	total emissions (%) <sup>a</sup>	max flux ( $\mu\text{g m}^{-2} \text{s}^{-1}$ )	max 24-h av ( $\mu\text{g m}^{-2} \text{s}^{-1}$ )	total emissions (%) <sup>a</sup>
<i>cis</i> -1,3-D	237	18	7.3	32	7.2	3.9	19	18	10	42
<i>trans</i> -1,3-D	237	12	4.9	23	4.4	2.6	13	9.2	6.1	28
chloropicrin	222	2.6	0.58	0.9	0.39	0.1	0.3	0.68	0.43	1.3

<sup>a</sup>Percent of total fumigant mass applied; assumes the flux rate is uniform within the field.

the experiment. During the daytime, the atmosphere was generally unstable (i.e.,  $\Phi_m < 1$ ). At night, lower wind speed and weaker buoyancy reduced mixing near the surface, allowing emission of gas to accumulate in concentration.

Fumigant concentrations were largest at the start of the experiment due to the high concentrations in the soil immediately following application, rapid diffusion due to soil fractures caused by the fumigation shanks and large initial gradients, and evaporation of fumigant from the injection rig to the atmosphere during application. This behavior was observed at all sampling distances (Figure 4) but is most easily interpreted for the on-field measurements, which were not influenced by wind direction and sample-station positions.

The off-site samples are particularly useful in determining emissions during the application process, before the on-field sensors could be installed. Application losses can occur when the fumigators lift the shanks from the soil as they turn for the next pass down the field. Although the injection valves are

closed to minimize waste and emissions, any residue remaining on the shank injectors and tubing evaporates into the atmosphere, increasing fumigant loadings. This is most noticeable at 30 m, during the first two sampling periods (Figure 4B) that were collected during fumigation and is a combination of application losses and losses from soil. The estimated mass lost during fumigation was <1% of applied.

Shank (i.e., a knife-like blade that cuts through soil with the injection nozzle at the lower end) injections tend to produce a more uniform concentration depth profile and higher concentrations near the soil surface compared to methods that do not produce a fracture,<sup>35</sup> but rapid movement along the shank fracture can lead to higher fumigant emissions. New application technology using a coultter and packer purports to reduce fumigant emissions and increase residue levels in soil,<sup>36</sup> on the basis of measurements collected at a depth of 12 cm. Further research is needed to obtain concentration distributions at other depths.

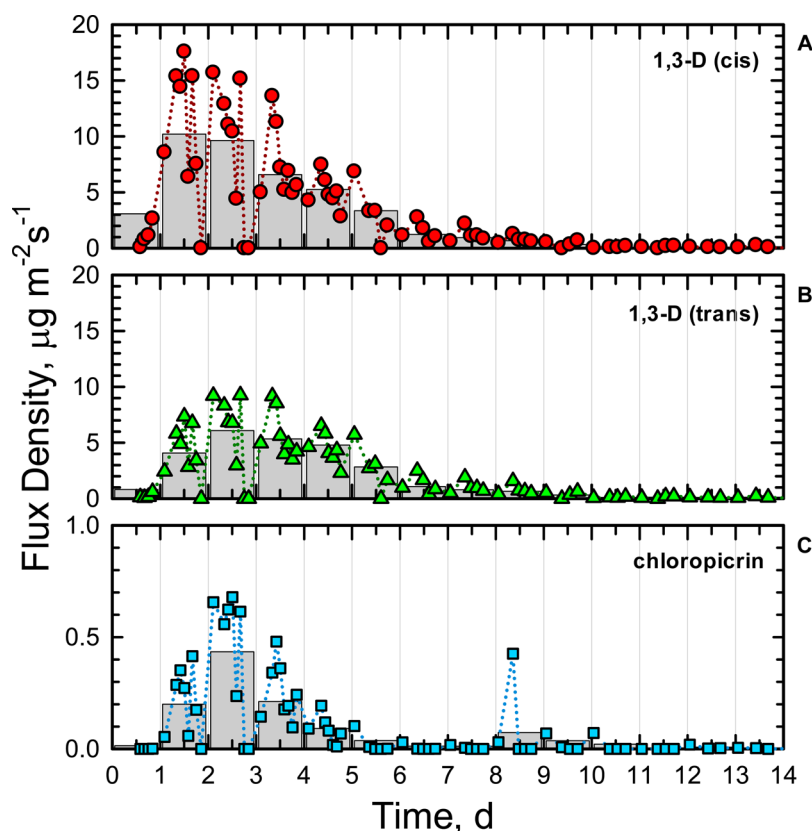


**Figure 6.** Volatilization rate (i.e., flux density,  $\mu\text{g m}^{-2} \text{s}^{-1}$ ) as a function of time (days) after application for the aerodynamic method. Shaded areas are mass losses for each day converted into daily averaged volatilization rates. For day 0, the shaded area is based on 16 h of available data.

The highest fumigant concentrations were measured near the field center, and progressively lower concentrations were observed at the more distant offsite sample stations. For example, the maximum period-averaged *cis*-1,3-D concentration during the experiment for on-field, 30, 60, and 120 m distances, respectively, were 1035, 112, 79, and 74  $\mu\text{g m}^{-3}$ . The overall behavior of *trans*-1,3-D was similar to that of *cis*-1,3-D, but with slightly lower concentrations (especially at early times). Compared to *cis*-1,3-D, *trans*-1,3-D is known to have an 8.2% higher boiling point (112.6 °C), 6.4% higher solubility (2320 ppm), 33% lower vapor pressure (23 mmHg), and 42% lower dimensionless Henry's law constant (0.037). In concert, these factors may result in a delay in *trans*-1,3-D movement to the soil surface, reduction in peak emission rates, and retardation of the peak emission timing.<sup>13,37</sup> Observed chloropicrin air concentrations were very low for all distances and times after chloropicrin application ended ( $t > 0.53$  day). The higher concentrations during fumigation were most likely due to the application process, as discussed above.

**Fumigant Emissions.** State and federal regulators are concerned about atmospheric loadings of soil fumigant chemicals, and information on emissions is used to estimate environmental risks and to determine risk related to acute bystander exposure. Information on the total emission rate is useful for determining contributions to regional volatile organic chemicals and for determining risks due to chronic exposure to fumigant chemicals.

The emissions of 1,3-D (*cis* + *trans*) calculated using ISCST3, CALPUFF (Figure 5), and ADM (Figure 6) methods demonstrate a similar overall pattern with higher rates early in the experiment and lower rates about 5–6 days post

application. The ISCST3 estimates were found to be consistently lower than estimates obtained using the CALPUFF model (53% lower on average). The largest differences occurred during the morning hours when the ISCST3 emissions were as much as 85% lower than the CALPUFF values. Using ISCST3, the reported total 1,3-D and chloropicrin losses, respectively, were 40 and 64% lower than the CALPUFF values.

During the first 5 days, the short-term volatilization rates follow a consistent cycle where the volatilization rate increases from midnight to midmorning, followed by a steep reduction in the volatilization rate at midday and low values until nighttime. This pattern is consistent with daytime drying of the surface soil, which leads to increased vapor adsorption. Increased adsorption reduces the pesticide vapor density and the vapor gradients,<sup>38–40</sup> which is an important transport mechanism. As water content in soil decreases below a threshold level, the reduction in vapor pressure would cause a reduction in pesticide emissions.<sup>41</sup> Using modeling, the effects of vapor adsorption have been shown to strongly bind volatile pesticides to soil particles in a highly nonlinear process.<sup>42,43</sup>

Whereas the emission measurements vary considerably with time of day, the long-term (e.g., daily averaged) emission rates (shaded areas in Figure 5) show a smoother and more predictable behavior that starts with a steady increase in the emission rate after fumigation, peaks on day 2, and is followed by a long period of decreasing emission rates. In terms of mathematically modeling the emission process, this behavior follows conventional transport theory.<sup>44</sup>

It can be shown that the timing of the maximum emission rate depends on the depth of injection<sup>35</sup> for a shank or point



fumigation (i.e., injection) model. This is due to the time needed for the fumigant to diffuse from the injection depth (46 cm) to the soil surface and volatilize into the atmosphere. For a shank fumigation using *cis*-1,3-D, the model predicts that the peak emission rate would occur at approximately 1–1.3 days after application, assuming a post fumigation soil-disking depth of 15–20 cm. This coincides with the experimental results using the on-field measurements (Figure 6) where the highest daily averaged emissions (shaded area) occur on day 1. For the CALPUFF method (Figure 5), the peak daily averaged emission rate occurs on day 2. It is unclear why the peak flux calculated from CALPUFF occurred at a later time than with the ADM method, but is probably due to differences in the approach for calculating flux values or the temporal nature of wind speed/direction, which are averaged over each sampling duration. For the ADM method, the sampling “footprint” (i.e., area of surface-soil-emissions captured by the sampling equipment) would be a relatively small zone immediately surrounding the sampling equipment, and the time period when the fumigant was injected into this area would have a relatively short duration. For the CALPUFF method, emissions over the entire field and transport from the field boundaries to the surrounding samplers affect the emission rate values. This means that the CALPUFF method could be affected by spatial and temporal averaging of the field emission rates and near-field transport processes.

In Figure 5, the first two flux values were measured during the fumigation period and demonstrate the gas losses occurring during application. Large emission losses during fumigation caused state regulators in California to restrict 1,3-D application from 1990 to 1995<sup>7</sup> to protect people living in fumigation areas. It was not until suitable application guidelines were developed and tested that use of 1,3-D was again allowed in California. During this experiment, losses during application were lower than emissions from soil that occurred later in the experiment and show that current regulations are effectively controlling losses during application.

A laboratory study<sup>45</sup> reported 1,3-D and chloropicrin emissions using Milham sandy loam soil collected from a nearby, nontreated, field in 2005. The stainless steel soil columns (1.5 m long) were placed in a controlled-temperature environment so that the columns were exposed to temperature conditions similar to those observed at the field site. The reported total *cis*-1,3-D emissions 14 days after treatment was 33.1% of applied. The emission rate from the laboratory experiment was within 1% of the CALPUFF *cis*-1,3-D total emission value.

In a follow-up experiment<sup>18</sup> that included 1,3-D and chloropicrin, the total 1,3-D (*cis* + *trans*) and chloropicrin emissions 14 days after injection, respectively, were reported as 40 and 16% of applied. The reported chloropicrin emission losses were much more than observed during this field experiment (e.g., ~1%). The soil at the field site was found to have relatively high soil degradation rates. Ashworth et al.<sup>18</sup> measured the 1,3-D and chloropicrin half-lives, respectively, as 90 and 2.9 h, at 25 °C. In a subsequent laboratory study Ashworth et al.<sup>46</sup> found that the chloropicrin degradation rate depended on the chloropicrin application rate, with low application rates leading to high degradation rates.

Rapid chloropicrin degradation in soil may have contributed to a reduction in soil concentration levels before sufficient time elapsed to allow significant volatilization, and to test this hypothesis, a mathematical model was used to predict total

emissions as a function of soil properties, injection depth, presence of a shank fracture, soil degradation, and surface resistance to volatilization.<sup>35</sup> A feasible explanation for the low chloropicrin emissions observed during the experiment is the soil degradation rate (i.e.,  $t_{1/2} = 2.9$  h), which led to predicted total emissions of <1%.

Very few large-scale field measurements of the emissions of 1,3-D and chloropicrin after broadcast application are reported in the literature. There are even fewer reported studies that utilize multiple methods for measuring the emission rate. This is due, in part, because conducting a field campaign is very expensive and requires large investments in time, equipment, and personnel. The current study is unique because it provides a continuous time series of the emissions for 14 days (daytime and nighttime) and involved collection of two independent data sets (i.e., on-field and off-field measurements). These data were then used so that the emission rate was calculated by three methodologies (i.e., ISCST3, CALPUFF, and ADM methods). Comparing the methodologies revealed that the increasing order of the total emissions was  $\text{ISCST3} < \text{CALPUFF} < \text{ADM}$ , and total emissions from CALPUFF are approximately the same as the average of the three methods.

Determining which method provides the most accurate emission rates is not possible with the data currently available, because there is no absolute reference for comparison. Each method encompasses inherent assumptions and/or simplifications that may affect the calculated values under some conditions. For example, ISCST3 is a steady-state atmospheric dispersion model, so results could be compromised for highly variable wind conditions during an hourly time step. CALPUFF is a non-steady-state Lagrangian puff model that tracks chemical movement in a more natural manner, a likely an improvement over ISCST3, but the results depend on the gridding system employed and the representativeness of the meteorological data. The ADM method assumes a well-developed surface layer for measuring gradients (concentration, wind speed, and temperature) and requires evaluation of a correction term for stable and unstable atmospheric conditions, which may introduce uncertainty. It is clear that further research is needed to better understand the accuracy and performance of these methods for calculating fumigant emissions.

Using total emissions from CALPUFF for comparison, the results of this study fall within the range of values reported in the literature for 1,3-D for similar application methodology (25–66%).<sup>24,36,47</sup> The results for chloropicrin were much different from emission values reported in the literature (i.e., 30–60%), which was attributed to the unusually high soil reactivity at the field site.

The results from this study should prove useful for conducting risk assessments. Recent U.S. EPA FIFRA Scientific Advisory Science Panels (SAP) conducted assessments of three fumigant bystander exposure models.<sup>48–50</sup> The SAP and model developers concluded that the availability of appropriate emission rate time series is critical to the effective use of these risk assessment models, because the emission rate defines the source term for fumigants in the airstream that can lead to exposures. Information on emission rates based on multiple and independent estimation methods, and that are applicable to field-scale conditions, provides valuable information for use in risk assessment.



## ■ ASSOCIATED CONTENT

### ■ Supporting Information

Schematic of the field site; description of the micrometeorological methods used in this study including a graph of the temperature difference, gradient Richardson's number, and atmospheric stability parameter; and graph of the soil water content data. The Supporting Information is available free of charge on the ACS Publications website at DOI: 10.1021/acs.jafc.5b01309.

## ■ AUTHOR INFORMATION

### Corresponding Author

\*(S.R.Y.) E-mail: scott.yates@ars.usda.gov. Phone: (951) 369-4803. Fax: (951) 342-4964.

### Present Addresses

<sup>Δ</sup>(W.Z.) Illinois Sustainable Technology Center, University of Illinois at Urbana-Champaign, Champaign, IL 61820, USA.

<sup>††</sup>(J.K.) FluxExperts, LLC, Carmel, IN 46032, USA.

### Funding

Part of the research described was supported by the California Air Resources Board (Agreement 05-351).

### Notes

The use of trade, firm, or corporation names in this paper is for the information and convenience of the reader. Such use does not constitute an official endorsement or approval by the U.S. Department of Agriculture or the Agricultural Research Service of any product or service to the exclusion of others that may be suitable.

The authors declare no competing financial interest.

## ■ ACKNOWLEDGMENTS

We are grateful to F. Ernst and J. Jobses for their assistance in preparing and conducting the reported experiment.

## ■ REFERENCES

- (1) van den Berg, F.; Kubiak, R.; Benjey, W.; Majewski, M.; Yates, S. R.; Reeves, G.; Smelt, J.; van der Linden, A. Emission of pesticides into the air. *Water, Air, Soil Pollut.* **1999**, *115*, 195–218.
- (2) Neal, R.; Spurlock, F.; Segawa, R. *Annual Report on Volatile Organic Chemical Emissions from Pesticides: Emissions for 1990–2007*; Report EH09-01 (March 2009); California Environmental Protection Agency: Sacramento, CA, USA, 2009; 39 pp.
- (3) Baker, L. W.; Fitzell, D. L.; Seiber, J. N.; Parker, T. R.; Shibamoto, T.; Poor, M. W.; Longley, K. E.; Tomlin, R. P.; Propper, R.; Duncan, D. W. Ambient air concentrations of pesticides in California. *Environ. Sci. Technol.* **1996**, *30*, 1365–1368.
- (4) Wauchope, R. D.; Buttler, T. M.; Hornsby, A. G.; Augustijn-Beckers, P. W. M.; Burt, J. P. The SCS/ARS/CES Pesticide properties database for environmental decision-making. *Rev. Environ. Contamin. Toxicol.* **1992**, *123*, 1–155.
- (5) Yates, S. R.; McConnell, L. L.; Hapeman, C. J.; Papiernik, S. K.; Gao, S.; Trabue, S. L. Managing agricultural emissions to the atmosphere: state of the science, fate and mitigation, and identifying research gaps. *J. Environ. Qual.* **2011**, *40*, 1347–1358.
- (6) Albrecht, W. N. Occupational exposure to 1,3-dichloropropene (Telone) in Hawaiian pineapple culture. *Arch. Environ. Health* **1987**, *42*, 286–291.
- (7) CDPR (California Department of Pesticides Regulation). California management plan: 1,3-dichloropropene; Department of Pesticide Regulation: Sacramento, CA, USA; <http://www.cdpr.ca.gov/docs/emon/methbrom/telone/mgmtplan.pdf>.
- (8) U.S. EPA. *Reregistration Eligibility Decision (RED) for Chloropicrin*; EPA 738-R-08-009; U.S. EPA Prevention, Pesticide and Toxic Substances: Washington, DC, USA, 2008; 128 pp.

(9) Carter, W. P. L.; Luo, D. M.; Malkina, I. L. Investigation of the atmospheric reactions of chloropicrin. *Atmos. Environ.* **1997**, *31*, 1425–1439.

(10) Wilhelm, S. N.; Shepler, K.; Lawrence, L. J.; Lee, H. Environmental fate of chloropicrin. In *Fumigants: Environmental Fate, Exposure, and Analysis*. ACS Symp. Ser. **1996**, No. 652, 79–93.

(11) Basile, M.; Senesi, N.; Lamberti, F. A study of some factors affecting volatilization losses of 1,3-dichloropropene (1,3-D) from soil. *Agric., Ecosyst. Environ.* **1986**, *17*, 269–279.

(12) Gan, J.; Yates, S. R.; Crowley, D.; Becker, J. O. Acceleration of 1,3-dichloropropene degradation by organic amendments and potential application for emissions reduction. *J. Environ. Qual.* **1998**, *27*, 408–414.

(13) Gan, J.; Yates, S. R.; Wang, D.; Ernst, F. F. Effect of application methods on 1,3-dichloropropene volatilization from soil under controlled conditions. *J. Environ. Qual.* **1998**, *27*, 432–438.

(14) Gan, J.; Yates, S. R.; Ernst, F. F.; Jury, W. A. Degradation and volatilization of the fumigant chloropicrin after soil treatment. *J. Environ. Qual.* **2000**, *29*, 1391–1397.

(15) Zheng, W.; Yates, S. R.; Papiernik, S. K.; Wang, Q. Q. Reducing 1,3-dichloropropene emissions from soil columns amended with thiourea. *Environ. Sci. Technol.* **2006**, *40*, 2402–2407.

(16) Gao, S.; Trout, T. J. Surface seals reduce 1,3-dichloropropene and chloropicrin emissions in field tests. *J. Environ. Qual.* **2007**, *36*, 110–119.

(17) McDonald, J. A.; Gao, S.; Qin, R.; Thomas, J. Thiosulfate and manure amendment with water application and tarp on 1,3-dichloropropene emission reductions. *Environ. Sci. Technol.* **2008**, *42*, 398–402.

(18) Ashworth, D. J.; Ernst, F.; Xuan, R.; Yates, S. R. Laboratory assessment of emission reduction strategies for the agricultural fumigants 1,3-dichloropropene and chloropicrin. *Environ. Sci. Technol.* **2009**, *43*, 5073–5078.

(19) van den Berg, F. Measured and computed concentrations of 1,3-dichloropropene in the air around fumigated fields. *Pestic. Sci.* **1992**, *36*, 195–206.

(20) van Wesenbeeck, I.; Knuteson, J. A.; Barnekow, D. E.; Phillips, A. M. Measuring flux of soil fumigants using the aerodynamic and dynamic flux chamber methods. *J. Environ. Qual.* **2007**, *36*, 613–620.

(21) Chellemi, D. O.; Ajwa, A.; Sullivan, D. Atmospheric flux of agricultural fumigants from raised-bed, plastic-mulch crop production systems. *Atmos. Environ.* **2010**, *44*, 5279–5286.

(22) Chen, C.; Green, R. E.; Thomas, D. M.; Knuteson, J. A. Modeling 1,3-dichloropropene vapor-phase advection in the soil profile. *Environ. Sci. Technol.* **1995**, *29*, 1816–1821.

(23) Chen, C.; Green, R. E.; Thomas, D. M.; Knuteson, J. A. Correction To: Modeling 1,3-dichloropropene vapor-phase advection in the soil profile. *Environ. Sci. Technol.* **1996**, *30*, 359.

(24) Gao, S.; Trout, T. J.; Schneider, S. Evaluation of fumigation and surface seal methods on fumigant emissions in an orchard replant field. *J. Environ. Qual.* **2008**, *37*, 369–377.

(25) Gao, S.; Qin, R.; Hanson, B. D.; Tharayil, N.; Trout, T. J.; Wang, D.; Gerik, J. Effects of manure and water applications on 1,3-dichloropropene and chloropicrin emissions in a field trial. *J. Agric. Food Chem.* **2009**, *57*, 5428–5434.

(26) Gao, F.; Yates, S. R.; Yates, M. V.; Gan, J.; Ernst, F. F. Design, fabrication, and application of a dynamic chamber for measuring gas emissions from soil. *Environ. Sci. Technol.* **1997**, *31*, 148–153.

(27) Ross, L. J.; Johnson, B.; Kim, K. D.; Hsu, J. Prediction of methyl bromide flux from area sources using the ISCST3 model. *J. Environ. Qual.* **1996**, *25*, 885–891.

(28) Barry, T. A.; Segawa, R.; Wofford, P.; Ganapathy, C. Off-site air monitoring following methyl bromide chamber and warehouse fumigations and evaluation of the Industrial Source Complex-Short Term 3 air dispersion model. In *Fumigants*; Seiber, J., et al., Eds.; ACS Symposium Series 652; American Chemical Society: Washington, DC, USA, 1996; pp 178–188.

(29) CDPR (California Department of Pesticides Regulation). Memorandum dated Aug 21, 2008 to Randy Segawa, Environmental

Monitoring Branch, Memorandum, Aug 21, 2008; [http://www.cdpr.ca.gov/docs/emon/pubs/ehapreps/analysis\\_memos/2071\\_segawa.pdf](http://www.cdpr.ca.gov/docs/emon/pubs/ehapreps/analysis_memos/2071_segawa.pdf).

(30) Johnson, B.; Barry, T.; Wofford, P. *Workbook for Gaussian Modeling Analysis of Air Concentration Measurements*; Report EH99-03; California Environmental Protection Agency: Sacramento, CA, USA, Sept 1999 (revised May 2010); 61 pp.

(31) U.S. EPA. *User's Guide for the AMS/EPA Regulatory Model – AERMOD*; EPA-454/B-03-001; U.S. Environmental Protection Agency: Research Triangle Park, NC, USA, 2004; 216 pp.

(32) Parmele, L. H.; Lemon, E. R.; Taylor, A. W. Micro-meteorological measurement of pesticide vapor flux from bare soil and corn under field conditions. *Water, Air, Soil Pollut.* **1972**, *1*, 433–451.

(33) Yates, S. R.; Knuteson, J.; Ernst, F. F.; Zheng, W.; Wang, Q. The effect of sequential surface irrigations on field-scale emissions of 1,3-dichloropropene. *Environ. Sci. Technol.* **2008**, *42*, 8753–875.

(34) Rosenberg, N. J.; Blad, B. L.; Verma, S. B. *Microclimate, The Biological Environment*; Wiley: New York, 1983; 495 pp.

(35) Yates, S. R. Analytical solution describing pesticide volatilization from soil affected by a change in surface condition. *J. Environ. Qual.* **2009**, *38*, 259–267.

(36) Chellemi, D. O.; Mirusso, J.; Ajwa, H. A.; Sullivan, D. A.; Unruh, J. B. Fumigant persistence and emission from soil under multiple field application scenarios. *Crop Prot.* **2013**, *43*, 94–103.

(37) Kim, J. H.; Mallavarapu, M. Isomeric effects on volatilization of 1,3-dichloropropene fumigant in soil. *J. Environ. Sci. Int.* **2009**, *18* (12), 1325–1330.

(38) Spencer, W. F.; Cliath, M. M.; Farmer, W. J. Vapor density of soil-applied dieldrin as related to soil-water content, temperature, and dieldrin concentration. *Soil Sci. Soc. Am. Proc.* **1969**, *33*, 509–511.

(39) Glotfelty, D. E.; Taylor, A. W.; Turner, B. C.; Zoller, W. H. Volatilization of surface-applied pesticides from fallow soil. *J. Agric. Food Chem.* **1984**, *32*, 638–643.

(40) Reichman, R.; Rolston, D. E.; Yates, S. R.; Skaggs, T. H. Diurnal variation of diazinon volatilization: soil moisture effects. *Environ. Sci. Technol.* **2011**, *45*, 2144–2149.

(41) Spencer, W. F.; Cliath, M. M. Pesticide volatilization as related to water loss from soil. *J. Environ. Qual.* **1973**, *2*, 284–289.

(42) Reichman, R.; Yates, S. R.; Skaggs, T. H.; Rolston, D. E. Effects of soil moisture on the diurnal pattern of pesticide emission: numerical simulation and sensitivity analysis. *Atmos. Environ.* **2013**, *66*, 41–51.

(43) Reichman, R.; Yates, S. R.; Skaggs, T. H.; Rolston, D. E. Effects of soil moisture on the diurnal pattern of pesticide emission: comparison of simulations with field measurements. *Atmos. Environ.* **2013**, *66*, 52–62.

(44) Jury, W. A.; Spencer, W. F.; Farmer, W. J. Behavior assessment model for trace organics in soil: 1. Model description. *J. Environ. Qual.* **1983**, *12*, 558–564.

(45) Ashworth, D. J.; Yates, S. R. Surface irrigation reduces the emission of volatile 1,3-dichloropropene from agricultural soils. *Environ. Sci. Technol.* **2007**, *41*, 2231–2236.

(46) Ashworth, D. J.; Yates, S. R.; van Wessenbeeck, I. J.; Stanghellini, M. Effect of co-formulation of 1,3-dichloropropene and chloropicrin on evaporative emissions from soil. *J. Agric. Food Chem.* **2015**, *63*, 415–421.

(47) Cryer, S. A.; van Wessenbeeck, I. J. Estimating field volatility of soil fumigants using CHAIN\_2D: mitigation methods and comparison against chloropicrin and 1,3-dichloropropene field observations. *Environ. Model Assess.* **2010**, *15*, 309–318.

(48) Cryer, S. A. Predicting soil fumigant air concentrations under regional and diverse agronomic conditions. *J. Environ. Qual.* **2005**, *34*, 2197–2207.

(49) Sullivan, D. A.; Holdsworth, M. T.; Hlinka, D. J. Monte Carlo-based dispersion modeling of off-gassing releases from the fumigant metam-sodium for determining distances to exposure endpoints. *Atmos. Environ.* **2004**, *38*, 2471–2481.

(50) Reiss, R.; Griffin, J. A probabilistic model for acute bystander exposure and risk assessment for soil fumigants. *Atmos. Environ.* **2006**, *40*, 3548–3560.